LUND UNIVERSITY

Impact of Band-Tails on the Subthreshold Swing of III-V Tunnel Field-Effect Transistor

Memisevic, Elvedin; Lind, Erik; Hellenbrand, Markus; Svensson, Johannes; Wernersson, Lars-Erik

Impact of Band-Tails on the Subthreshold Swing of III-V Tunnel Field-Effect Transistor

Elvedin Memisevic,[a] Erik Lind, M. Hellenbrand, J. Svensson, and Lars-Erik Wernersson

Department of Electrical and Information Technology, Lund University, 221 00 Lund, Sweden

[a]Electronic mail: elvedin.memisevic@eit.lth.se

We present a simple model to evaluate the sharpness of the band edges for tunnel field-effect transistors by comparing the subthreshold swing and the conductance in the negative differential resistance region. This model is evaluated using experimental data from InAs/InGaAsSb/GaSb nanowire tunnel-field effect transistors with the ability to reach a subthreshold swing well below the thermal limit. A device with the lowest subthreshold swing, 43 mV/decade at 0.1 V, exhibits also the sharpest band-edge decay parameter E_0 of 43.5 mV although in most cases the $S<<E_0$. The model explains the observed temperature dependence of the subthreshold swing.

I. INTRODUCTION

Tunnel Field-Effect Transistors (TFET) are a promising steep slope transistor candidate for future low power electronics. TFETs rely on band-to-band tunneling (BTBT), also known as Zener tunneling, to filter out the high energy tail of the source

1

carriers. To achieve a low subthreshold swing (S), a TFET requires sharp band edges and low amount of defect-induced states within the band gap [1-3], as well as a low level of interface defects. Experimental observation of states inside the band gap are thus of importance.

Measurements on two terminal Esaki diodes require heavily doped p^+n^+-junctions, whereas an nTFET will be designed with a p^+-i-n structure. The heavier doping profile in the diode may result in a different distribution and amount of traps as well as disorder induced band tails as compared to the TFET [4-6]. Thereby, measurements on diodes only are of limited use. We here present a simple model for evaluating the band edge sharpness from measurements on TFETs, which relates the conductance in the negative differential resistance (NDR) region to the subthreshold swing. The model is evaluated on TFETs with S<60 mV/decade. We also find that the model well reproduces the experimentally observed temperature dependence of the subthreshold swing of the TFETs.

II. Model and Devices

Figure 1a-b shows schematic band diagrams for a heterostructure TFET in the off-state (a) and an Esaki diode negative differential resistance (NDR) region (b). The lowest channel conduction sub-band ($E_{c,ch}$) is above the source valence band ($E_{v,s}$). For an ideal device, BTBT between the $E_{v,s}$ and $E_{c,ch}$ would start when a bias is applied so $E_{c,ch}$ reaches a level below $E_{v,s}$. In a real device, the existence of energy states in the band gap (defects and/or band tails) will open an alternative current path, trap assisted tunneling (TAT). For normal TFET off-state operation ($V_{DS} > 0$ V, $V_{GS} < V_T$), charges are thermally

excited to the band gap states, constituting a generation current, from where they can tunnel into the channel as shown in Fig 1a. This effect will impact the device subthreshold swing.

The NDR region of the TFET with V_{SD} larger than the peak voltage, corresponding to Fig. 1b will also be influenced by band gap states. In this process, charges in the channel will tunnel to states in the bandgap and subsequently recombine with holes in the source, forming a recombination current. This is typically called excess current for an Esaki diode [7-9]. In the steepest NDR region for devices with sufficiently high peak-to-valley current ratio, we typically find the current to decrease exponentially with increasing source voltage. This can be described phenomenologically by an exponentially decreasing set of band gap states close to the source valence band edge, characterized by an energy decay parameter E_0. While this is similar to models of the Urbach tail, the states considered here may also be induced from local defects [10]. We model the off-state (excess current) for a single 1D sub band tunneling current and current using equation 1

$$(1) \qquad I_{D,off} = \kappa \frac{2q}{h} \int_{E_c}^{\infty} T_r(E)(f_d - f_s) \exp\left(-\frac{E}{E_0}\right) dE$$

where T_r is the tunneling transmission, f_d/f_s the drain/source distribution functions, and κ a constant which models the concentration of states within the band. For Urbach tails we expect $\kappa \approx 1$, whereas defect induced states can have different values. For simplicity we here use $\kappa = 1$. Here, any states in the band gap are projected to the InAs/InGaAsSb heterostructure interface, at which position they will have largest impact. For the off-state in Fig. 1a, as only charges in the Fermi-tail are involved we use the

Boltzmann approximation to replace the Fermi-Dirac functions in (1) and further assume a large V_{DS} and energy independent T_r, which is essentially valid for a homojunction TFET. For a heterostructure TFET T_r is expected to increase with energy. The estimated value of E_0 thus includes both the effects of the band tail states as well as the voltage dependence of the tunneling probability. Equation 1 then simplifies to

$$(2) \qquad I_{D,off} \approx \frac{2q}{h} T_r \int_{E_c}^{\infty} \exp\left(-\frac{E}{E_0}\right) \exp\left(\frac{E_{Fs}-E}{kT}\right) dE \propto \exp\left(-\frac{E_0+kT}{E_0 kT} E_c\right).$$

Using (2) subthreshold swing can be written as:

$$(3) \qquad S = \left(\frac{d\log(I_{D,off})}{dV_g}\right)^{-1} = 2.3 \frac{kTE_0}{kT+E_0}\left(1 + \frac{C_{it}}{C_{ox}}\right),$$

where the last term originates from effects due to interface traps, relating the movement of the sub band to the applied gate voltage, as given by equation 4. Thus, for a TFET with an off-current limited by exponentially decreasing band tails, the ideal S is lower than 60 mV/decade, as long as the device is operating in the exponential region of the Fermi-tail. Interface defects will then further degrade S. For a TFET with transport involving band states with thermal population that limit the subthreshold swing, we thus expect a change in S with temperature.

$$(4) \qquad \frac{-\delta E_C}{\delta V_g} = \frac{q}{1+\frac{C_{it}}{C_{ox}}}$$

The current in the NDR away from the peak region can also be estimated from equation 1. Assuming $V_{DS} > 100$ mV and a large enough gate voltage, the channel becomes degenerate, as indicated in Fig 1b, for which we can approximate

$$(5) \qquad I_S \approx \frac{2q}{h} T_r \int_{E_c}^{E_{F,S}} \exp\left(-\frac{E}{E_0}\right) dE \sim \exp\left(-\frac{qV_s}{E_0}\right).$$

In the last step we use that the source valence band is shifted by qV_s and assumed degenerate channel conditions so that $E_{f,d} \gg E_{c,d}$. The value of E_o can be determined by fitting (5) to the exponential part of the NDR region as shown in Fig. 1d. The subthreshold swing is thus affected by E_0, kT and C_{it}, whereas the NDR directly probes E_0.

Several devices from three different samples (Sample A, Sample B, and Sample C) where used to determine S and E_0. A large majority of the devices exhibit a S below 60 mV/decade, data for one device is presented in Fig, 1c. For Sample A and Sample C the composition of the vertical nanowires is InAs/In$_{0.1}$Ga$_{0.9}$As$_{0.88}$Sb$_{0.12}$/GaSb with lengths of 200/100/300 nm and the thinnest diameter (InAs channel region) 20 nm. The physical gate-length is 150 nm and the number of the nanowires varies from one to eight. In Sample C, the whole InAs section is n-doped (10^{18} cm^{-3}), while in Sample A, the top half of the InAs-section is undoped. The composition of the vertical nanowires on Sample B is InAs/In$_{0.32}$Ga$_{0.68}$As$_{0.72}$Sb$_{0.28}$/GaSb with the same dimensions and doping profile as nanowires on Sample A. Further information about the fabrication and properties of these devices can be found in [11, 12]. The gate-currents are two to three orders lower than lowest channel currents.

III. DISCUSSION

In Fig. 2a, data from a device on Sample A is shown, with a highest PVCR of 10.4 and a S of 53 mV/dec. The value of E_0 is 56-59 meV, determined using Eq. 6 for two different V_{GD}. E_0 is determined in the region showing exponential current change. It

may hence be an underestimate of the distribution function as direct BTBT still contribute in this bias region and the exact shape will depend on the detailed tail density of states. In Fig. 2b, S vs E_0 from several devices from Samples A and B are presented. The mean D_{it} is about $(2-9) \cdot 10^{12}$ eV^{-1}cm^{-2} which is similar to values from CV measurements [13]. Devices consisting of more than one nanowire typically show a larger estimated E_0, which we attribute to random V_T and nanowire diameter ensemble variations, leading to a larger estimated extrinsic E_0.

Data from the devices from both samples are well described by the simple model. Data for a device from Sample C is presented in Fig 2c, these devices have a doping profile similar to a diode with doping on both sides of the heterojunction. These devices show a substantially larger valley current. Using the gate-terminal, PVCR can be increased from 4.73 to 7.6 with increasing V_{GD}. This action will increase channel charge and thus increase the BTBT current modeled here as well as screen the potential around impurities. Thereby the value of the estimated E_0 is lowered from 114 meV to 78 meV. Furthermore, the device S is 77 mV/decade. In our devices, estimates of E_0 from measurements on Esaki-type p+n+ yield limited information for p+-i-n type TFETs.

Figure 2d shows the temperature dependence for S and E_0 for two devices from Sample A and two devices from Sample B. The model reproduces the measured data well down to T ~ 100 K. For very low temperature (T=11K), the modeled S is found to be lower as compared with measurements. This difference can originate from non-thermal effects not included here, such as direct (or trap assisted) source to drain tunneling, or self-heating.

E_0 does not show any strong temperature dependence, and is found to be about 50-60 meV for all temperatures. This makes phonon induced band tails as the fundamental origin of the band gap states improbable. Instead, discrete dopants and their fluctuations (37 meV activation energy for Zn in GaSb) and impurities (Urbach tails), as well as defect induced band gap states are the probable sources for the excess current. The typical source doping is about 10^{19} cm^{-3}, which is similar to the valence band density of states, which supports the use of k≈1. A similar argument can be made for the InAs channel.

To verify the approximation done in Eqs 2 and 5, we have numerically calculated the tunneling current, by integrating Eq.1 in addition to a direct BTBT model. We have here utilized a simple 2-band WKB-model with simple constant electric field [14] for the transmission calculations, set by the device geometric length scale. As shown in Fig. 3a and b, using E_0 and the threshold voltage as fitting parameters, a good agreement between measured and modeled data is achieved. The fitted $E_0 = 54$ meV agrees well with 59 meV which was evaluated directly from the NDR slope. This indicates that the omission of the energy dependence in $T_r(E)$ does not cause a too large error in the estimation of E_0.

IV. CONCLUSIONS

A simple model has been introduced which captures the essential role of band tails in the off-state and NDR region of TFETs. The proposed model can well reproduce the temperature dependence of the subthreshold swing of TFETs. Results from experimental data shows that a device with $E_0 > 60$ meV can still achieve a subthreshold

swing below 60 mV/decade. Decreasing the amount of traps, as well as reducing the decay parameter E_0 will be required to achieve even lower subthreshold swing.

ACKNOWLEDGMENTS

[1]   S. Agarwal and E. Yablonovitch, "Band-Edge Steepness Obtained From Esaki/Backward Diode Current-Voltage Characteristics", *IEEE Electron Device Lett.*, vol.61, no. 5, pp. 1498 - 1493, May 2014, DOI: 10.1109/TED.2014.2312731

[2]   R. N. Sajjad, W. Chern, J. L. Hoyt, and D. A. Antoniadis, "Trap assisted tunneling and its effect on subthreshold swing of tunnel field effect transistor", *IEEE Trans. Electron. Dev.,* vol. 63, no. 11, pp. 4380-4387, Nov. 2016 DOI: 10.1109/TED.2016.2603468

[3]   H. Lu, D. Esseni, and A. Seabaugh, "Universal analytic model for tunnel FET circuit simulation", *Solid-State Elect.,* vol. 108, no. -, pp. 110-117, Jan. 2015, DOI: 10.1016/j.sse.2014.12.002

[4]   J. N. Schulman and D. H. Chow, "Sb-Heterostructure Interband Backward Diodes" *IEEE Electron Device Lett.* , vol. 21, no. 7, pp. 353 – 355, July 2000, DOI: 10.1109/55.847378

[5]   H. Riel, K.E. Moselund, C. Bessire, M. T. Björk, A. Schenk, H. Ghoneim, and H. Schmid, *"InAs-Si Heterojunction Nanowire Tunnel Diodes and Tunnel FETs"* in *Int. Electron Device Meeting (IEDM),* Dec. 2012, 391-394, DOI: 10.1109/IEDM.2012.6479056

[6]   P. Thomas, M. Filmer, A. Gaur. D. J. Pawlik, B. Romanczyk, S. L. Rommel, K. Majumdar, W. -L. Loh, M. H. Wong, C. Hobbs, K. Bhatnagar, R. Contreras-Gurrero, and R. Droopad, "Perforamce Evaluation of $In_{0.53}Ga_{0.47}As$ Esaki Tunnel Diodes on Si and InP substrates ", *IEEE Trans. Electron. Dev.*, vol. 62, no. 8, pp. 2450-2456, Augusti 2015, DOI: 10.1109/TED.2015.2445731

[7]   A. G. Chynoweth, W.L. Feldmann, and R. A. Logan, "Excess Tunnel Current in Silicon Esaki Junctions", *Phys. Rev.*, vol. 121, no. 3, pp. 684-694, February 1961, DOI: 10.1103/PhysRev.121.684

[8]   J. A. Del Alamo and R. D. Swanson, "Forward-Bias Tunneling: A limitation to bipolar device scaling", *IEEE Electron Device Lett.*, vol. 7, no. 11, pp. 629-631, November 1986 DOI: 10.1109/EDL.1986.26499

[9]   C. D. Bessire, M. T. Björk, H. Schmid, A. Schenk, K. B. Reuter, and H. Riel, "Trap-assisted Tunneling in Si-InAs Nanowire Heterojunction Tunnel Diodes", *Nano Lett.*, vol. 11, no. 10, pp. 4195-4199, August 2011, DOI: 10.1021/nl202103a

[10]   M. A. Khayer and R.K. Lake, "Effects of band-tails on the subthreshold characteristics of nanowire band-to-band tunneling transistors", *J. Appl. Phys.*, vol. 110, no. 7, pp. 074508-1 - 074508-1, October 2011, DOI: 10.1063/1.3642954

[11]   E. Memisevic, J. Svensson, M. Hellenbrand, E. Lind, and L.-E. Wernersson, "Vertical InAs/GaAsSb/GaSb tunneling field-effect transistor on Si with S = 48 mV/decade and I_{on} = 10 µA/µm for I_{off} = 1nA at V_{DS} = 0.3 V", in *Int. Electron*

Device Meeting (IEDM), Dec. 2016, 500-503, DOI: 10.1109/IEDM.2016.7838450

[12]   E. Memisevic, M. Hellenbrand, E. Lind, A. R. Persson, S. Sant, A. Schenk, J. Svensson, R. Wallenberg, L.-E. Wernersson, "Individual Defects in InAs/InGaAsSb/GaSb Nanowire Tunnel Field-Effect Transistors Operating below 60 mV/decade", *Nano Lett.*, vol. 17, no. 7, pp. 4373-4380, May 2017, DOI: 10.1021/acs.nanolett.7b01455

[13]   J. Wu, A. S. Babadi, D. Jacobsson, J. Colvin, S. Yngmann, R. Timm, E. Lind, and L.-E. Wernersson, "Low Trap Density in InAs/High- k Nanowire Gate Stacks with Optimized Growth and Doping Conditions", *Nano Lett.*, vol. 16, no. 4, pp. 2418-2425, March 2016, DOI: 10.1021/acs.nanolett.5b05253

[14]   E. Lind, E. Memiseivic, A.W. Dey, and L.-E. Wernersson, "III-V Heterostructure Nanowire Tunnel FETs", *IEEE J. Elec. Dev. Soc.*, vol. 3, no. 3, pp. 96-102, April 2015, DOI: 10.1109/JEDS.2015.2388811

Figure Captions

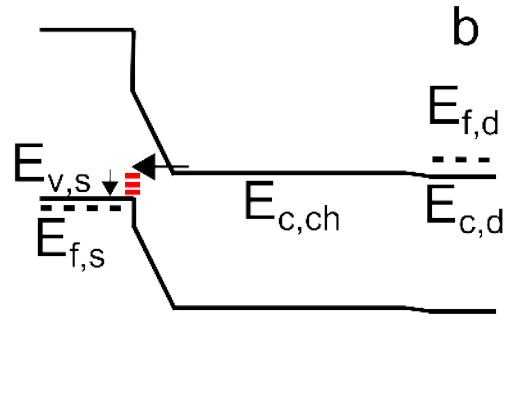Figure 1. (a) Schematic band diagram for a heterostructure TFET in the off-state. (b) Schematic band diagram for an Esaki diode negative differential resistance. (c) Transfer curve from a TFET from Sample B with S = 46 mV/decade at 50 mV. (d) NDR from output data from device in Fig 1c. Dotted red line is fitted to determine value of the E_0. Insert shows same data and fit plotted with linear scale.

Figure. 2. (a) NDR in output data from a device from the Sample A at two different V_{GD}. The value of E_0 is not changing with V_{GD}. (b) S vs E_O for a number of devices from Sample A and Sample B. Black symbols represent devices with one nanowire, whereas colored symbols correspond to devices with 2-8 nanowires. The D_{it} used in Eq. 3 is $6 \cdot 10^{12}$ eV^{-1}cm^{-2}. (c) NDR in output data from a device from Sample C at two different V_{GD}. The value of E_0 decreases with increasing PVCR. With a high PVCR the impact of excess current is lower. (d) Temperature dependence of S. Data is from 2 devices from Sample A and from 2 devices from Sample B. Every device is represented by its own color. The D_{it} used in Eq. 3 is $6 \cdot 10^{12}$ eV^{-1}cm^{-2}. The insert shows the temperature dependence of the E_0.

Figure 3. Using the model, fitting is performed on experimental data. (a) Transfer curve of a device. (b) Fitting to the NDR region in the output data. Used values are: E_0 = 54 meV, dE$_V$=0.15 E$_{fs}$ = 100 meV, E$_{gs}$= 58 meV. D_{it} = $1.4 \cdot 10^{12}$ eV^{-1}cm^{-2}

a

$E_{v,s}$

$E_{f,s}$

$E_{c,ch}$

$E_{f,d}$

$E_{c,d}$

Source   Channel   Drain

b

$E_{f,d}$

$E_{v,s}$

$E_{c,ch}$

$E_{c,d}$

$E_{f,s}$

Source   Channel   Drain

c

$I_D(\mu A/\mu m)$

V_{GS} (V)

2 NW

V_{DS} = 50 mV

S_{MIN} = 46 mV/dec.

d

$I_S(\mu A/\mu m)$

V_{SD} (V)

Eq. 6

E_0 = 62 meV

Panel a:

Sample A

V_{GD} = 0.2 V
V_{GD} = 0 V

a

I_S (μA/μm)

I_{peak} = 1.56 μA/μm
(31 kA/cm^2)
PVCR 10.4

I_{peak} = 0.68 μA/μm
(13.6 kA/cm^2)

PVCR 7.55 E_0 = 56.3 meV
E_0 = 59.8 meV
S_{MIN} = 53 mV/dec.

V_{SD} (V)

Panel b:

(Const. T_r is assumed)

b

S_{MIN} (mV/dec)

1 NW >1 NW
Sample A
Sample B
Eq. 3 w/o influence of D_{it}
Eq. 3 with influence of D_{it}

E_0 (meV)

Panel c:

Sample C

c

I_S (μA/μm)

I_{peak} = 7.05 μA/μm
(141 kA/cm^2)
PVCR 7.6

I_{peak} = 2.9 μA/μm
(58 kA/cm^2)
PVCR 4.73

V_{GD} = 1 V
V_{GD} = 0.6 V

E_0 = 78 meV
E_0 = 114 meV
S_{MIN} = 77 mV/dec.

V_{SD} (V)

Panel d:

Sample A Sample B
Eq. 3 w/o influence of D_{it}
Eq. 3 with influence of D_{it}
(Const. T_r is assumed)

d

S_{MIN} (mV/dec)

E_0 (meV)

Temperature (K)

Temperature (K)